LOAN DOCUMENT

PHOTOGRAPH THIS SHEET

DTIC ACCESSION NUMBER

LEVEL

INVENTORY

Image Processing for LADAR Automatic...

DOCUMENT IDENTIFICATION

1999

DISTRIBUTION STATEMENT A
Approved for Public Release
Distribution Unlimited

DISTRIBUTION STATEMENT

**H
A
N
D
L
E
W
I
T
H
C
A
R
E**

DATE ACCESSIONED

DATE RETURNED

20010201 050

DATE RECEIVED IN DTIC

REGISTERED OR CERTIFIED NUMBER

PHOTOGRAPH THIS SHEET AND RETURN TO DTIC-FDAC

DTIC FORM 70A
JUN 90

DOCUMENT PROCESSING SHEET

LOAN DOCUMENT

PREVIOUS EDITIONS MAY BE USED UNTIL
STOCK IS EXHAUSTED.

Image Processing for LADAR Automatic Target Recognition[†]

Alan Van Nevel
Larry Peterson
Charles Kenney
Naval Air Warfare Center, China Lake, CA 93555
vannevelaj@navair.navy.mil
petersonla@navair.navy.mil
kenneycr@navair.navy.mil

Abstract

In this paper we present a novel synthesis of image processing algorithms which enable high performance in an ATR system for ladar seekers. Ladar data presents both unique capabilities and problems for image processing. We will discuss unique approaches to incorporate the three dimensional nature of the data, while handling range dropouts and the ground plane background in a manner that allows for robust ATR performance.

1. Introduction and Background

Laser radar (or ladar) sensors have been receiving increased attention in recent years, as sensor systems continue to improve, and may make a tactical ladar sensor feasible. The desirability of ladar sensors arises from several different factors. First and foremost, the nearly three dimensional nature of the data, and the high resolution of detail that ladar sensors can provide holds great promise for improved capabilities, such as target/object recognition, terrain navigation, and aim-point selection. In addition, while ladar sensors are an active system, the emissions are much more focussed and shorter range, making it more difficult to detect.

Given the unique nature of data that is provided by current ladar sensors, novel image processing techniques are required to make full use of the information contained within the ladar data. To this end, we have developed and/or implemented four advanced algorithms, which when working in concert, provide an improved system performance for automatic target recognition. The algorithms perform four very different tasks. The first task is noise removal and mitigation, which is performed by a filtering process called Peer Group Averaging (PGA)[1,2]. Following noise mitigation is an unique visualization transform which also allows convenient correlation processing[3]. The correlation processing is performed using MACH filters[4-10]. A final task, which could be performed at any point in the processing stream, is image segmentation using total variational approaches[11-16]. All of these algorithms will be covered in detail in the following sections.

2. Peer Group Averaging

2.1 Ladar Noise

While sensor noise can and does contribute to degradation of range image quality, the most noticeable effect are range dropouts . These occur when a pixel does not receive enough energy to trigger a valid range detection. This effect often results from atmospheric attenuation of the laser beam or absorption by a surface. While the nature of the noise can be very dependent upon how the sensor handles dropouts, most sensors return a very large or very small value for the range associated with a dropout pixel. An example image contaminated by a large number of dropouts can be seen in Figure 1. The noise often is a hurdle that must be overcome when simply trying to visualize the data. The dynamic range of the sensors in question is 16 bit, and while the true data may only lie in a narrow range band, the noise often will cover the full 16 bit range, which can be difficult to visualize.

2.2 Peer Group Averaging

Kenney *et al* have introduced a new non-linear approach to image enhancement known as peer group averaging (PGA)[1,2]. It is a scheme based on the idea that each pixel has a peer group of associated nearby

pixels. The peer group is then used to modify the value of the target pixel.

Peer group defined: For an image (or signal) **g**, the peer group **P**(n,r) associated with pixel i consists of the n pixels within the distance r of i that are nearest in intensity to **g**(i) . Peer group averaging is the process of replacing **g**(i) with the average over its peer group **P**(n,r).

PGA is a stable algorithm which converges quickly. While it is a non-linear algorithm which makes a general convergence proof difficult, approximations can be made for limited PGA approaches. For a longer discussion on convergence see Kenney *et al* [2] . In addition to the quick convergence of the PGA algorithm, it has other properties which make it desirable for image enhancement. Depending on the choice of window radius r and peer group number n , a tradeoff between edge preservation and noise removal can be made. In addition, the algorithm can be implemented in an adaptive and multiscale method, giving greater flexibility in terms of noise removal and image enhancement. Some examples of PGA filtering on images can be seen in Figures 2a-c.

3. Visualization Transforms

As mentioned in the previous section, visualizing ladar data can be somewhat difficult due to the large dynamic range of the data. PGA filtering mitigates the range dropouts, which reduces the effective dynamic range, but not enough so that detail is easily seen in the raw range data. Some sort of transform is needed that reduces the dynamic range, takes advantage of the three dimensional nature of the data, and produces an image which preserves all the detail available in the original data.

Often, researchers attempt to remove the ground plane when dealing with ladar range imagery. The background provides a nearly linear gradient on which objects of interest sit. If one could effectively remove the ground plane, what remains could be considered potential objects of interest for correlation based processing. The projective transform [3] we have implemented renders the background plane to a near constant value, placing it on an equal footing with potential targets for correlation based processing.

The transform we use to accomplish all of these goals is actually rather simple. To take advantage of the three dimensional information, one calculates a surface normal for every pixel in the range image. Following this calculation, a virtual point light source location is chosen (azimuth and elevation), and a dot product between the pixel surface normal and the light source vector is

taken. One can interpret the result as the intensity image that would result given a light source and a uniform reflectance for all pixels in the image. In addition, the dot product also lends insight to how the surfaces are oriented with respect to the virtual light source.

Some results of the projective transform can be seen in Figures 3a-c. The transform can be performed as a visualization tool, producing color (RGB) imagery, or as a preprocessing step, resulting in gray scale imagery. The new imagery now is scaled to {0,1}, and the background plane is now near a constant value.

4. MACH Filters

4.1 Introduction and Theory

Mahalanobis, Kumar *et al* [4-12] have recently introduced an advanced family of correlation filters known as maximum average correlation height (MACH) filters. The use of MACH filters for automatic target recognition (ATR) has been motivated by the properties of the MACH filters. Since MACH filters are a correlation filter, they can be implemented easily and operate at high rates of speed given current hardware processing speeds. The biggest hurdle in the past for any correlation filter was the number of templates that needed to be processed in order to cover a large range of aspect and scale changes. MACH filters overcame this deficiency by providing improved distortion tolerance. For example, using some previous correlation approaches for SAR data, one may have used one template for every 4 degrees of aspect, resulting in 90 templates for full aspect coverage. In contrast, Mahalanobis [12] has demonstrated excellent results using one template every 30 degrees, a 7 fold reduction in the number of templates needed. The tolerance of the filters is incorporated through the selection of an appropriate training set, and can be tuned to provide high (generalization) or low (specificity) tolerance.

In the discussion of the MACH filters that follows, bold lowercase indicates a column vector, while bold uppercase represents a diagonal matrix. The filters result from maximizing the ratio

$$J(\mathbf{h}) = \frac{\left|\mathbf{h}^+\mathbf{m}\right|}{\mathbf{h}^+\mathbf{S}\mathbf{h}} \qquad (1)$$

where **h** is the correlation filter and **m** is the average of the training images in the Fourier domain. Each image is lexigraphically ordered to form a vector. **S** is the average similarity measure matrix

$$S = \sum_{k=1}^{N} (\mathbf{X}_k - \mathbf{M})(\mathbf{X}_k - \mathbf{M})^{+}. \qquad (2)$$

In eq. (2) $\mathbf{X}_k$ are the individual training images, again in the Fourier domain. The training image is lexigraphically ordered and its elements placed on the diagonal of $\mathbf{X}_k$ while $\mathbf{M}$ is the mean training image, arranged similarly to $\mathbf{X}_k$. Furthermore, all of the processing to generate the filters is performed in the Fourier domain to gain translational invariance. It is possible to perform the processing in other domains (*e.g.* wavelet or spatial) but care must be taken to properly register the training imagery.

The optimal filter $\mathbf{h}$ is then given by

$$\mathbf{h} = \mathbf{S}^{-1}\mathbf{m}. \qquad (3)$$

Variants on the MACH filter can be achieved by varying the performance metric one wishes to maximize. For example Refrieger [8] has developed optimal trade-off synthetic discriminant filters (OTSDF's) which attempt to minimize the energy functional

$$E(\mathbf{h}) = \mathbf{h}^{+}\mathbf{Q}\mathbf{h} - \delta|\mathbf{h}^{+}\mathbf{m}| \qquad (4)$$

where

$$\mathbf{Q} = \alpha\,\mathbf{P} + \beta\,\mathbf{D} + \gamma\,\mathbf{S}. \qquad (5)$$

$\mathbf{S}$ is as defined previously, $\mathbf{P}$ is the power spectral density of the expected noise, and $\mathbf{D}$ is the average power spectral density of the training set. The constants $\alpha, \beta, \gamma, \delta$ are non-negative and must satisfy $\alpha^2 + \beta^2 + \gamma^2 + \delta^2 = k$ where k is any positive constant. Minimizing $E(\mathbf{h})$ results in

$$\mathbf{h} = \frac{\delta}{2}\mathbf{Q}^{-1}\mathbf{m}. \qquad (6)$$

By varying the parameters, one can optimize filter performance for the situation under study. If one sets $\alpha = \beta = 0$, the result is the MACH filter discussed earlier. Further variations can be made to the basic idea, including the extension to multiple class discrimination using distance classifier correlation filters [6] (DCCF's), which are able to distinguish between multiple classes of similar objects (*e.g.* T72's vs. M1A1 tanks).

The class of MACH filters (which includes OTSDF's and DCCF's) was chosen for the feature detection for several reasons. As discussed, the filters can incorporate varying degrees of distortion tolerance and can be built to generalize classes of targets. Another benefit of the algorithm is that the result is statistically optimum and depends on a realistic, mathematically rigorous optimaztion procedure as opposed to other heuristic methods. A final consideration is the computational efficiency. The MACH filters require no segmentation or edge detection preprocessing and the correlation step can be performed rapidly using dedicated FFT hardware.

4.2 MACH implementation

To implement the MACH filters, one must first decide upon a representative training set. Typically, the training set consists of N<20 images from varying perspectives. A training set of one image will result in a filter similar to the matched filter with no distortion tolerance while having dozens of perspectives and scalings will produce a filter with a broad response and low discrimination properties. The filter $\mathbf{h}$ is first calculated off-line from the training data. If one is using the OTSDF's, some parameter tuning can be done at this point to maximize the correlation peaks for the training data.

Following correlation of an input test scene with $\mathbf{h}$, the correlation scene must be processed to determine the areas of interest. Previous correlation filters had placed constraints on the correlation height, and classification was then accomplished by comparing the correlation height of the test scenes to the constraint. Generally, when using the correlation height as a metric for detection and/or classification, a threshold must be set. By changing this threshold one can trade off between the probability of detection and the probability of false alarms, a lower threshold allowing more false alarms and a higher threshold reducing the probability of detection.

A second metric that is more stable and generally yields better results is known as the peak to side lobe ratio (PSR). Given a correlation peak p the PSR is given by

$$PSR = \frac{p - \mu}{\sigma} \qquad (7)$$

where μ is the mean within an annulus around the peak, and σ is the standard deviation in the annulus. Typically one uses an inner radius of a few pixels (1-4) and an outer radius of 6 or more pixels, depending on the application. The benefit of this approach is that the ratio is independent of illumination or amplification effects. The overall peak height can be affected by constant amplification but the ratio will remove this problem. This metric works well in rejecting false peaks due to clutter since most correlation surfaces for clutter images will not contain a high percentage of energy in a localized window.

When dealing with ladar range images, the biggest factor in designing the MACH filters is how to choose the training set. Preliminary clustering analysis indicates that the data varies much more rapidly with range rather than aspect. This indicates that large aspect changes can be grouped into one training set if one keeps the range variance small. In our experiments, the aspect range of the training sets was typically 20 degrees in azimuth, and the range variance was between 60 and 200m. Given a test image, a mean range reference was calculated and used to select the appropriate range filter.

5. Variational Image Segmentation

While the MACH filter does not require image segmentation to deliver adequate performance, and within our system the projective transform has removed the linear bias of the ground in the raw range image, image segmentation at the appropriate time in the processing stream may improve system performance. Since ladar sensors provide range measurements, it is possible to calculate size estimates of objects in an image, given an accurate segmentation. The size estimates can be used to cull possible false detections based on expected sizes of targets, and this process can be performed at any point in the processing stream.

Much has been written in the literature for image segmentation [13-16], and a wide variety of approaches exist. The approach we have chosen to use is a variational formulation of image segmentation. The approach is to minimize an energy functional which measures three different properties,

$$E(u,b) = \omega_1 \int (u-g)^2 \, dx + \omega_2 \int |\nabla u|^p \, dx + \omega_3 \int db \quad (6)$$

where u is the segmentation approximation to the image (measuring fidelity to original image g). The second term measures the smoothness of the approximation, while the third term measures the length of all region boundaries. In practice, a model for u is chosen beforehand. The models most commonly used are piecewise constant, piecewise linear, and piecewise quadratic. Piecewise constant is often used since the second term becomes zero and does not contribute to the energy functional. The ω_1, ω_2, ω_3 are weights applied to each term, and can be used to determine a scale space decomposition of the image [14].

In our application, rather than try to determine an ideal set of weights, an adaptive procedure was adopted, whereby a set number of segmented regions was specified. The segmentation was applied to both the raw range imagery, using a piecewise linear or quadratic

model, or to the projective transformed data, using a piecewise constant model. Each method seemed to yield visually acceptable results. Examples of segmented images can be seen in Figures 4a-c.

6. Computer Experiments and Results

6.1 Data Set and Experiment Parameters

As mentioned earlier, ladar sensors are currently being considered for new tactical weapon systems, as ladar range images are thought to provide more information. Our goal was to integrate the image processing algorithms in attempt to demonstrate ATR capabilities for ladar range data. The dataset that is available for testing consists of over 440 passes of captive flight tests. Each pass consists of on the average ten images. The imagery contains small mobile targets or fixed large targets. The number of targets may vary from as few as four to more than twenty, and the type of clutter varies from no or light clutter to heavy clutter. The images in Figures 3a-d show the types of targets and clutter that are present in the imagery. Parts of this data may be available from www.vdl.afrl.af.mil . Since this research effort is geared to algorithm development rather than system evaluation, the data set used for testing and evaluation was limited to five different passes of the same target site with different approach angles. Within this limited set there were over 1000 target detection opportunities.

For the experiments that follow, the MACH filters were tuned to match the approximate aspect orientation of the target data. In one pass, the aspect orientation was 110 degrees (near broadside view), and the MACH filters used to process this pass were generated using training data from 92 to 112 degrees. The filters for the other four passes used were similarly trained, where the test data aspect orientation was near the limits of the training data aspect ranges. While this experimental set up does not attempt to demonstrate that full aspect coverage , the results are promising enough to merit further efforts toward a full evaluation of MACH filtering for ladar ATR. At the time these experiments were performed, only one synthetic target type, an M60 tank, was available to generate training data and the results shown are for detecting M60 tanks or other tank like vehicles.

As noted in the previous sections, each of the algorithms used has their own parameter set. While it is our eventual goal to characterize this ATR approach, considering as wide a variety of parameter combinations and the resulting ATR performance, for this work we will discuss some of the common values used for each preprocessing step. In the PGA noise removal, a small

3x3 pixel window was used, with a peer group of 6 or less. These parameters have the effect of removing dropouts from the range data, preserving edges in the data, and the processing runs in a reasonable amount of time. No other parameter sets for PGA were used. The projective visualization transform has two parameters, the angular location of the virtual light source (azimuth and elevation). In this case, parameter selection was based upon visual inspection. Due to an imbalance in the ladar sensor used to collect data, a striping effect could be seen in the range data, and the projection transform parameters were selected to minimize this effect in the transformed data. Other parameter choices were considered, but did not indicate that higher ATR performance would be realized.

The MACH filters and the scoring algorithms for the correlation plane have several parameters, and each one could have a profound impact on the overall detection performance. In building a MACH filter, there are three parameters α, β, and γ to be chosen. The first controls how heavily the mean of the training data is weighted, and also any noise suppression. The second and third parameters control the shape of the correlation output. A high β value will force much the correlation plane to a delta function, requiring a close match between test and training data, while a high γ value will allow more distortion by constraining the correlation plane to a specific shape determined by the training data. A wide variety of parameters were used, and the results will note which particular set was used.

Once a correlation plane is generated, scoring and detection takes place. The PSR (eq. 7) is calculated for a local correlation peak using two parameters (the inner window diameter and the outer window diameter). This generates a list of potential detections which is compared to a PSR threshold. All three of these parameters vary with regard to range and other parameter values. Typical window diameters range from 3 to 8 pixels for the inner window and 8 to 30 pixels for the outer diameter. The threshold varies between 5 and 12 and often changes with range, as more pixels on target yield a higher PSR.

Finally, use of the segmenter requires a choice of algorithmic approach (piecewise constant or linear) and an estimate of the number of segmented regions. If raw range data was segmented, the segmentation algorithm used a piecewise linear approach, otherwise piecewise constant was used. The number of regions varied with the range of the data, longer range data being segmented in more regions. Long range data (2000m) was segmented into approximately 100 regions, while for close range data (800m) the number of regions selected was 30.

6.2 Experiments, Results and Conclusions

The actual experiment was rather limited in scope. Given the first three processing steps (noise removal, projective transform, and MACH filtering) determine whether both an acceptable probability of detection, P_d and probability of false alarm, P_{fa}, could be achieved. Following this, image segmentation was considered as an additional processing step, either as a preprocessor screening regions of interest in the image based on target size, or as a postprocessor screening detections passed by the MACH filter based on size.

Given a data pass, the approximate aspect orientation of the targets was known and a corresponding synthetic training set was generated that covered the range variance of the pass. Following training set generation, a set of MACH filters were built with approximately 20 degrees of aspect tolerance (test aspect was chosen to be at the end of the training range), and 120m of range tolerance. This amount of distortion tolerance results in 13 filters being used to process one pass.

Each frame of test data undergoes preprocessing as described in the previous sections. First PGA for noise removal and image smoothing, followed by the projective transform. The next step is MACH filtering and scoring of the correlation plane. Use of the segmenter was limited to use as a postscreener, eliminating potential target detections based on size of the segmented region. As will be seen in the results, applying the segmenter in this fashion yielded unsatisfactory results. This is due to the possible under- or oversegmentation of potential targets. If a target vehicle is oversegmented into too many smaller regions, the screening will eliminate valid detections as being too small, while undersegmentation will group the target into a larger background region, again eliminating valid detections as being too large.

Table 1 indicates the performance of the ATR system for detection of M60 tanks. The first column reflects the percentage of M60 tanks correctly detected over the entire pass under study. The number of M60's in each frame of a particular pass varies from frame to frame. At long ranges, there are up to 14 M60 tanks visible in the scene, while at close range only 4 tanks are visible. The second column is the average number of confusers detected per frame. Any vehicle that is not an M60 is labeled a confuser. Future work will distinguish between different confuser types, in order to better characterize the algorithm. The third column is the average number of clutter false alarms per image. Each row of data refers to a particular pass and parameter set. As expected an inverse relationship is seen between detection rates and false alarm rates.

On the average, detection rates were above 90% which is a minimum acceptable threshold. The false alarm rate seen in this experiment may be considered high, and more work needs to be done to reduce the number of false alarms. Use of the segmenter as a prescreener, using liberal values for approximate sizes of potential targets will be one approach considered. PGA filtering does appear to increase detection results, but only when the test data is very noisy. Under consideration is adapting PGA to take advantage of knowledge of the seeker. In terms of improving confuser recognition, the tests will be expanded to contain more vehicle classes, and the filter set will also expand to include DCCF's to perform discrimination between similar classes.

In this work we have demonstrated the feasibility of using MACH filters for LADAR ATR. The success of the MACH filters was enabled using a unique combination of image processing techniques adapted to ladar imagery. MACH filters have been shown to provide an adequate level of performance both in terms of detection probability and in terms of false alarm occurrences while dramatically reducing the number of filters needed for traditional correlation based processing.

References

[1] Y. Deng, C. Kenney, M. Moore, B.S. Manjunath,"Peer Group Filtering and Perceptual Color Image Quantization," *Proc. IEEE Int. Symp. Circuits and Systems*, Vol 4 pp. 21-24, 1999.

[2] C. Kenney,G. Hewer,Y. Deng,and B.S. Majunath, "Peer Group Image Processing,", ECE Technical Report, University of California-Santa Barbara, Nov. 1999.

[3] S. Chang, M. Rioux, J. Domey, "Face recognition with range images and intensity images," *Optical Engineering*, vol. 36 #4, pp1106-1112, 1997.

[4] D. Carlson, "Optimal tradeoff composite correlation filters," Ph.D. thesis Carnegie Mellon Univ., Oct. 1996.

[5] A. Mahalanobis *et al*, "Unconstrained correlation filters," *Applied Optics*, vol. 33, pp. 3751-3759, 1994.

[6] A. Mahalanobis, B.V.K. Vijaya Kumar, and S.R.F. Sims, "Distance classifier correlation filters for multiclass target recognition," *Applied Optics*, vol. 35, pp. 3127-3133, 1996.

[7] B.V.K. Vijaya Kumar, D. Carlson, and A. Mahalanobis, "Optimal tradeoff synthetic discriminant function (OTSDF) filters for arbitrary devices," *Optics Letters*, vol. 19, pp. 1556-1558, 1994.

[8] Ph. Refregier, "Optimal tradeoff filters for noise robustness, sharpness of the correlation peak and Horner efficiency," *Optics Letters*, vol.16, pp. 829-831, 1991.

[9] Z. Bahri and B.V.K. Vijaya Kumar, "Generalized synthetic discriminant functions," *J. Opt. Soc. Am. A*, vol. 5, pp. 562-571, 1988.

[10] B.V.K. Vijaya Kumar, "Minimum variance synthetic discriminant functions," *J. Opt. Soc. Am. A*, vol.3, pp. 1574-1584, 1986.

[11] A. Mahalanobis, B.V.K. Vijaya Kumar, and D. Casasent, " Minimum average correlation energy filters," *Applied Optics*, vol. 26, pp 3633-40, 1987.

[12] A. Mahalanobis, D. Carlson, B.V.K. Vijaya Kumar,"Evaluation of MACH and Dccf Filters for SAR ATR using the MSTAR public database,",*Proc. of the SPIE*, Vol 3370, pp460-8, 1998.

[13] J. Morel and S. Solimini,*Variational Methods in Image Segmentation,* Birkhauser, Boston 1995.

[14] D. Mumford and J. Shah,"Optimal Approximation by Piecewise Smooth Functions and Associated Variational Problems," *Comm. On Pure and Appl. Math,* Vol XLII, no 4, 1989.

[15] G. Hewer, C. Kenney, and B.S. Manjunath,"Variational Image Segmentation Using Boundary Functions," *IEEE Trans. On Image Proc.*, Vol 7, no. 9, pp1269-1282, Sept 1998.

[16] G. Hewer, C. Kenney, L.Peterson, A. Van Nevel, "PDE Techniques for Variational Image Processing,"*Proc. of ICIP*, pp372-375, 1997.

[17] www.vdl.afrl.af.mil Cruise Missile Real Time Retargetting (CMRTR) LADAR Collection.

Figure 1. Sample range image showing range dropouts as dark pixels

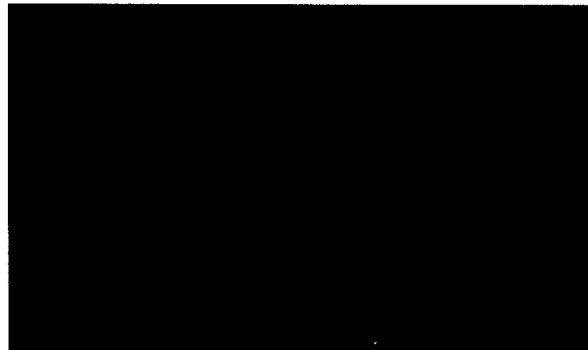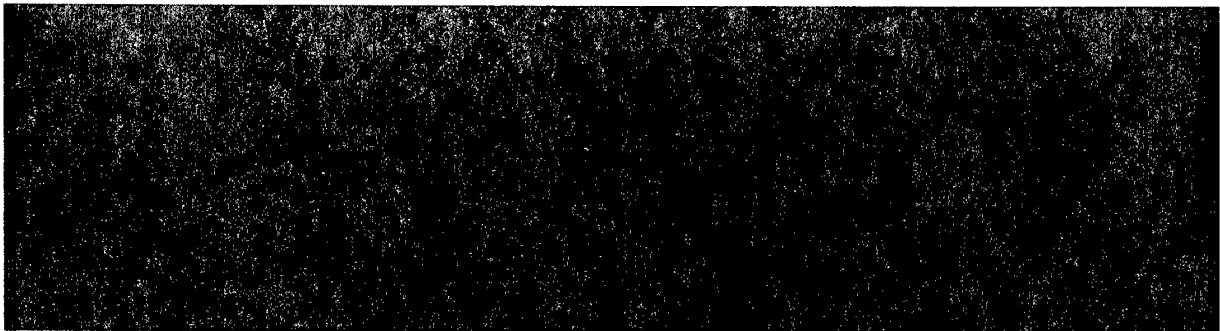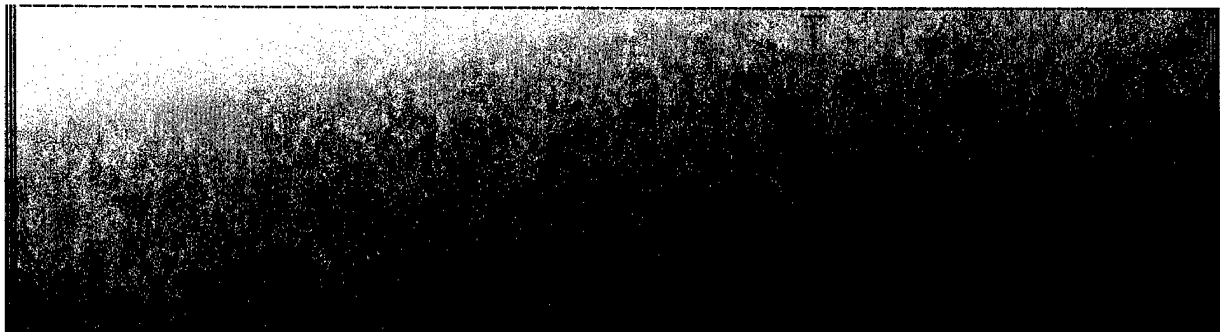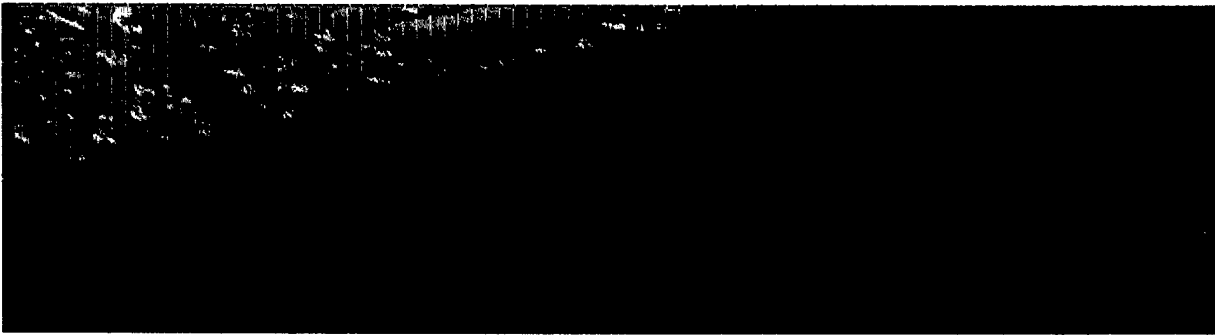**Figure 2a.** Result of PGA processing on image in figure 1
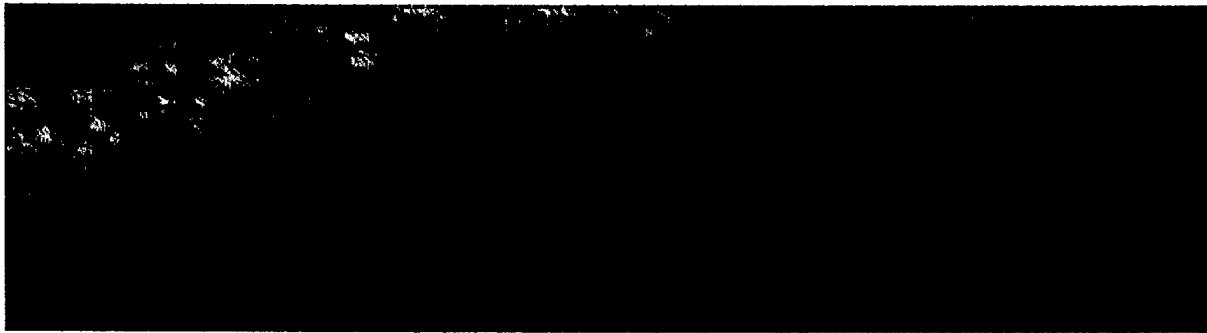

(b)

(c)

Figures 2b-c. Original raw range image (b) and PGA processing result (c).
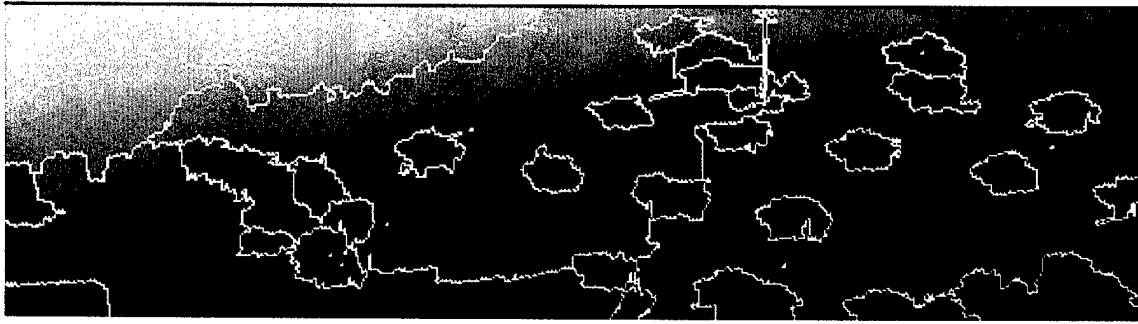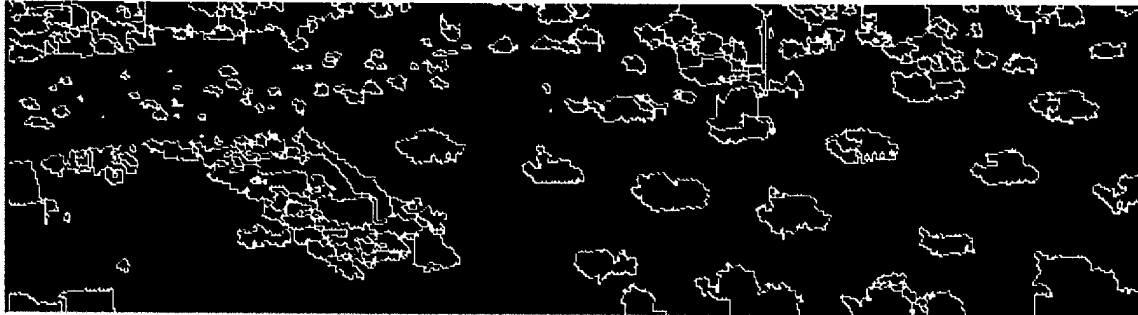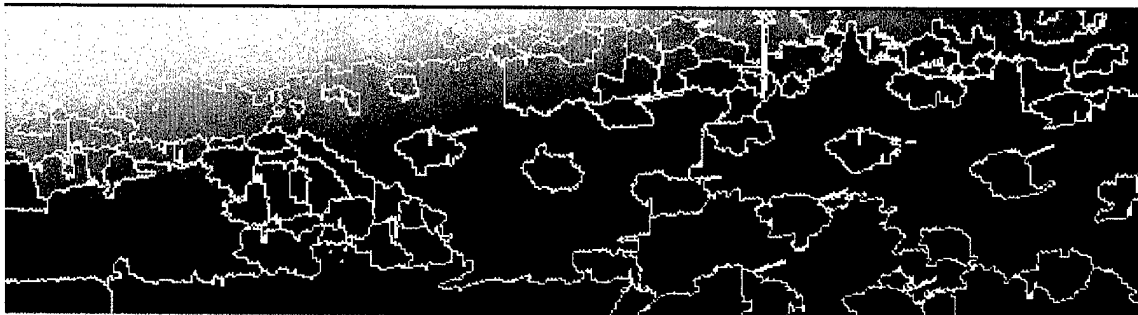
(a)

(b)

(c)

Figures 3a-c. Images showing the results of visualization transform. Images depict desert scrub clutter with a variety of target vehicles.

(a)

(b)

(c)

Figures 4a-c. Range imagery with segmentation boundaries overlaid

	M60's detected	Confusers per image	False Alarms per image
Parameter set 1	81.0%	2.5	0.32
Parameter set 2	96.4%	5.3	6.1
Parameter set 3	86.2%	2.2	1.1
Parameter set 4	91.7%	2.1	3.9

Table 1. Detection rates for M60 tanks in ladar data.

Computer, Megahertz	Execution time				
	ODE	LU	Sparse	3-D	2-D
This computer	0.22	0.13	0.25	1.11	0.52
DEC Alpha, 600	0.70	0.30	0.43	0.94	0.73
Pentium II, NT, 400	0.76	0.46	0.44	1.61	1.19
Pentium II, Linux, 400	0.65	0.42	0.52	1.72	1.19
SGI Octane, 195	1.10	0.43	0.60	1.63	1.19
Pentium II, Win98, 350	0.84	0.51	0.50	1.34	1.85
Sparc Ultra 2, 300	0.82	0.60	0.66	1.73	1.31
Pentium II Laptop, NT, 266	1.02	0.67	0.64	1.78	2.50
Pentium Pro, Linux, 200	1.21	0.83	1.05	2.45	1.57
HP 780, 180	1.69	0.46	1.13	2.83	2.24
IBM RS6000, 167	1.42	0.50	0.77	3.39	2.98
Sparc 10, Dual 160	2.12	1.07	1.29	4.50	3.08
SGI O2, 180	2.52	1.73	1.60	3.99	2.62
Sparc 2 (circa 1992)	10.00	10.00	10.00	10.00	10.00

ORIGINAL

Session 9

Government Disclosure Authorization Form

Disclosure authorization is required for all presentations. If this form is not received prior to the meeting the presentation will be canceled.

PART I

Name of Author(s) *Alan Van Nevel, Charles Kenney, Larry Peterson*

Title of Paper: *Image Processing for LADAR ATR*

Classification of Paper/Presentation (circle one)   SECRET   CONFIDENTIAL   (UNCLASSIFIED)

Author's Signature: *Al J - S Nevel*

****

PART II RELEASING OFFICIAL

Name of Releasing Official: BRAD HARLOW

Title: HEAD, WEAPONS SYSTEMS ENGINEERING DIVISION CODE 471000D

Address: 1 ADMINISTRATION CIRCLE, CHINA LAKE, CA 93555-6100

Telephone Number: (760)939-2529

The Releasing Office, with the understanding that all attendees have current security clearances and that all attendees have approved need-to-know certification, and that no foreign national will be present, confirms that the overall classification of this paper is UNCLASSIFIED   and authorizes disclosure at the meeting.

Classified by:_____   Declassify on:_____

Distribution Statement: _____

Releasing Official's Signature: _____

ORIGINAL

REQUEST FOR PUBLIC RELEASE OF UNCLASSIFIED INFORMATION   00-033

INSTRUCTIONS

1. Submit original and 3 copies plus paper/presentation (1 copy for 4B0000D; 1 copy for 750000D; 1 copy for 741100D; and 1 copy for author). Author is responsible to retain the record copy and attachments.

Session 9

FROM	CODE	TELEPHONE NUMBER	DATE NEEDED
Alan Van Nevel	471600D	939-1440	ASAP

1. Release is required for the attached material. This paper is related to a China Lake project.

2. The sponsor has consented to this release.

NAME OF SPONSOR	ORGANIZATION	TELEPHONE NUMBER
Tom Loftus	NAWCWPNS	(760) 939-3544

TITLE (Paper, presentation/speech, contractor release, patent, etc.)
MACH Filters and Projective Transforms for LADAR Automatic Target Recognition

TYPE
☐ PAPER   ☐ PRESENTATION/SPEECH   ☐ CONTRACTOR RELEASE   ☐ PATENT   ☒ OTHER____ abstract

MEETING OR PUBLICATION	PLACE/DATE OF MEETING OR RELEASE DATE	INITIALS	
AIAA Missile Science Conf.	Nov 7-9, 2000, Monterrey CA	AUTH	SPVSR

		INITIALS	
3. It is my opinion that the subject matter in this material has no information or military application requiring classification.		AVN	
4. To the best of my knowledge, this material does not disclose any trade secrets or suggestions of outside individuals or concerns that were communicated to China Lake in confidence.		AVN	
5. I reviewed the appropriate sections of the Military Critical Technology List (MCTL) and judge that the information does not contain military critical technology.		AVN	

AUTHOR'S COMMENTS

Abstract submission

AUTHOR'S SIGNATURE	DATE
	02-03-00

ROUTING	APPROVED	DIS-APPROVED	DATE	COMMENTS
DEPARTMENT HEAD CODE:			3/8/00	
CHAIRMAN, PUBLIC TECHNICAL INFORMATION RELEASE PANEL CODE: 4B0000D			3/2/00	MCTL ✓
CODE: 741100D			3/4/00	
CODE: 750000D			3/8/00	

NAWCWPNS OL 5720/3 (5-95)   (All previous revisions are obsolete)